

Charge Pumping and Photovoltaic effect in Open Quantum Dots.

Maxim G. Vavilov and V. Ambegaokar

Laboratory of Atomic and Solid State Physics, Cornell University, Ithaca, NY 14853

Igor L. Aleiner

Department of Physics and Astronomy, SUNY at Stony Brook, Stony Brook, NY 11794

(November 12, 2018)

We propose a random matrix theory to describe the influence of a time-dependent external field on electron transport through open quantum dots. We describe the generation of the current by an oscillating field for the dot, connected to two leads with equal chemical potentials. For low frequency fields our results correspond to adiabatic charge pumping. Finite current can be produced if the system goes along a closed loop in parameter space, which covers a finite area. At high frequency a finite current is produced even if the loop is a line in parameter space. This result can be explained in the same way as adiabatic pumping but considering the evolution of the system in phase space rather than in parametric space.

PACS numbers: 73.23.Ad, 72.15.Rn, 72.70.+m

I. INTRODUCTION

Adiabatic charge pumping through open quantum dots was studied recently in the literature both theoretically [1–3] and experimentally [4]. Such pumping occurs in a system described by a Hamiltonian periodic in time with a period T_p larger than all other characteristic time scales of the system. After one period, the system returns to its initial form; however charge Q can be transmitted through a cross-section of the system:

$$Q = I_{DC}T_p = \int_0^{T_p} \langle I(t) \rangle dt, \quad (1)$$

where $\langle \dots \rangle$ denotes quantum mechanical and thermodynamic averaging.

To obtain a finite transmitted charge at low frequencies, the Hamiltonian should depend on at least two parameters. In Refs. [1–3] the time dependence of the Hamiltonian was replaced by a dependence on parameters and the system was considered quasistationary for each parameter value. The transported charge during one period of the Hamiltonian was calculated as an integral in the parameter space. The theory [3] shed some light on the recent experiments [4], namely on the amplitude dependence of the root mean square fluctuations of the transmitted charge, averaged over different realizations of the Hamiltonian.

A very similar phenomenon was considered previously by Falko and Khmelnitskii, who theoretically studied the photovoltaic effect in mesoscopic microjunctions [5]. The experimental observation is described in Ref. [6]. The photovoltaic effect is a generation of d.c.-current by radiation of a finite frequency. (It is obvious that this effect can only be non-linear in the oscillating field.) The bilinear regime of adiabatic pumping, [1–3] is precisely the circular photovoltaic effect introduced in Ref. [7] and applied to a mesoscopic system in Ref. [5]. The results of

Ref. [5] are not directly applicable to quantum dots because in microjunctions the Thouless energy $E_T \sim 1/\tau_{\text{erg}}$ is of the same order as the inverse escape time $1/\tau_{\text{esc}}$, whereas for quantum dots $1/\tau_{\text{esc}} \ll E_T$. (Here τ_{erg} is the characteristic time for a classical particle to cover all of the available phase space in the dot and we put $\hbar = 1$.) Therefore the considerations of Refs. [1,3] have their own physical significance. On the other hand, the theory of Ref. [5] is not restricted to the adiabatic regime, the results being valued in a broad interval of frequencies.

The purpose of the present work is to go beyond the adiabatic approximation for d.c.-current generation in open quantum dots. One can identify two contributions to the d.c.-current — reversible and irreversible. To make a connection with the terminology of the photovoltaic effect, used in Ref. [5], we consider the bilinear d.c.-current response through the dot, generated by several time-dependent perturbations $\varphi_i(t) = \varphi_{i,\omega} e^{i\omega t}$.

The direct current I_{DC} can be written at $\omega \rightarrow 0$ as

$$I_{DC} = i\omega \epsilon_{ij} \varphi_{i,\omega} \varphi_{j,\omega}^* + \omega^2 \gamma_{ij} \varphi_{i,\omega} \varphi_{j,\omega}^* + \mathcal{O}(\omega^3), \quad (2)$$

where ϵ_{ij} and γ_{ij} are real sample specific coefficients. They are not fixed by any symmetry (a sample does not have any!) except the condition that I_{DC} is a real number, which gives the requirements

$$\epsilon_{ij} = -\epsilon_{ji}, \quad \gamma_{ij} = \gamma_{ji}. \quad (3)$$

These relations mean that as the direction of the contour in the parameter space $\{\varphi_i(t)\}$ is reversed ($\varphi_i(t) \rightarrow \varphi_i(-t)$ or $\varphi_{i,\omega} \rightarrow \varphi_{i,\omega}^*$), the first term changes its sign whereas the second term remains intact. In the language of the photovoltaic effect, the first term is the circular photovoltaic effect, and the second term is the linear effect. [5] Equation (2) makes an explicit connection between the bilinear responses of d.c.-current generation through open quantum dots and the photovoltaic effect.

We will see that the separation onto reversible and irreversible parts goes far beyond the bilinear and low frequency expansions. We will find that the reversible part vanishes at high frequency whereas the irreversible part saturates. We will also show that the irreversible contribution may be interpreted in a manner similar to adiabatic pumping. In adiabatic pumping the transmitted charge was determined by a contour in parameter space. The irreversible current is determined by the contour in the extended phase space $\{\varphi_i(t), \dot{\varphi}_i(t), \dots\}$, see Sec. V.

The first term in Eq. (2) vanishes for a single pump due to the antisymmetry of ϵ_{ij} , Eq. (3). The contour in parameter space degenerates to a line in this case, while in phase space the contour encompasses a finite area. We will see that the current is proportional to this area. Note, that the contour is invariant with respect to time inversion.

The remainder of the paper is organized as follows. In section II we formulate the model which is studied in the paper. We mainly discuss the high temperature limit $T \gg \omega$, where ω is the frequency of the perturbation. In section III we calculate the ensemble averaged fluctuations of the current. As an example, low frequency asymptotic of reversible (adiabatic) and irreversible currents are considered. In Sec. IV we discuss how the irreversible contribution can be represented in the form of a linear integral over the contour in extended phase space. In Sec. V we discuss the low temperature limit and show how to take heating into account. Section VI summarizes our results.

II. THE MODEL

We consider the following experimental realization of the model. Gates near a two-dimensional electron gas (2DEG) form the shape of the dot. An oscillating voltage is applied to the gates $V_1(t)$ and $V_2(t)$. As a result of motion of electron energy levels in the dot, a current flows through the dot. The direction of the current depends on the particular realization of the dot and is zero on average. We calculate the fluctuations of the d.c.-current with respect to different realizations of the dot.

Calculations will be performed for an open quantum dot in the limit of a large number of open channels N_{ch} connecting the dot to the leads. This condition allows us to neglect the electron-electron interaction, which gives corrections of the $1/N_{\text{ch}}^2$ order, (See Ref. [8]). The same condition permits the use of a diagrammatic technique, similar to that described in [9], to calculate ensemble averaging.

We also assume that the quantum dot is small and the Thouless energy $E_T \sim 1/\tau_{\text{erg}}$ is much greater than all other energy scales of the problem. In this limit, one

can use random matrix theory (RMT) to study transport and thermodynamic properties of the system, see Ref. [10]. All corrections to the RMT are as small as $N_{\text{ch}}/g_{\text{dot}}$, where $g_{\text{dot}} = E_T/\delta_1$, δ_1 is the mean level spacing. We neglect the fluctuations of the time dependent perturbation from sample to sample, created by the voltages $V_{1,2}(t)$, since they depend on the small parameter $g_{\text{dot}}^{-1} \ll 1$.

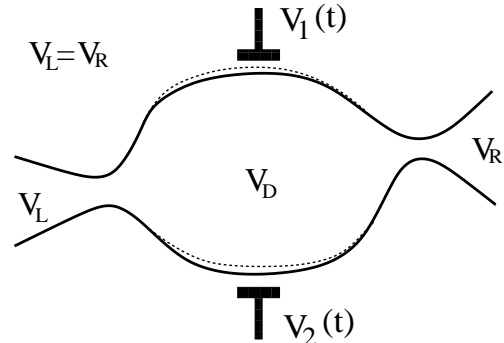


FIG. 1. An experimental setup. The voltage applied to the gates $V_1(t)$ and $V_2(t)$ changes the shape of the dot, resulting in motion of the energy levels of the electrons in the dot.

The Hamiltonian of the system is [10]

$$\hat{H} = \hat{H}_D + \hat{H}_L + \hat{H}_{LD}, \quad (4)$$

where \hat{H}_D is the Hamiltonian of the electrons in the dot, which is determined by the $M \times M$ matrix H_{nm} :

$$\hat{H}_D = \sum_{n,m=1}^M \psi_n^\dagger H_{nm} \psi_m, \quad (5)$$

where the thermodynamic limit $M \rightarrow \infty$ is assumed.

The coupling between the dot and the leads is

$$\hat{H}_{LD} = \sum_{\alpha,n,k} (W_{n\alpha} \psi_\alpha^\dagger(k) \psi_n + \text{H.c.}), \quad (6)$$

where ψ_n corresponds to an electron state in the dot, $\psi_\alpha(k)$ denotes electron state (α, k) in the leads, and k labels the continuum of momentum states in each channel α . For a dot connected by two leads with N_l and N_r channels respectively, we denote the left lead channels by $1 \leq \alpha \leq N_l$ and the right channels by $N_l + 1 \leq \alpha \leq N_{\text{ch}}$, where $N_{\text{ch}} = N_l + N_r$. The coupling constants, $W_{n\alpha}$, in Eq.(6) are [10]:

$$W_{n\alpha} = \begin{cases} \Gamma_n, & \text{if } n = \alpha \leq N_{\text{ch}}, \\ 0, & \text{otherwise} \end{cases} \quad (7)$$

and Γ_n are defined below in Eq. (19)

The electron spectrum in the leads near Fermi surface can be linearized

$$\hat{H}_L = v_F \sum_{\alpha,k} k \psi_\alpha^\dagger(k) \psi_\alpha(k), \quad (8)$$

where $v_F = 1/2\pi\nu$ is the Fermi velocity, and ν is the density of states per channel at the Fermi surface.

The current through the dot is given in terms of the scattering matrices $\hat{S}(t, t')$ by the following expression, see appendix A:

$$\langle I(t) \rangle = e \sum_{\alpha} \Lambda_{\alpha\alpha} \int dt_1 dt_2 \quad (9)$$

$$\times \left\{ \sum_{\beta} \mathcal{S}_{\alpha\beta}(t, t_1) f_{\beta}(t_1 - t_2) \mathcal{S}_{\beta\alpha}^{\dagger}(t_2, t) - f_{\alpha}(+i0) \right\},$$

where $f_{\alpha}(t)$ is the Fourier transform of the electron distribution function in the leads, $\langle \dots \rangle$ stands for the quantum mechanical and thermodynamic averages for a given ensemble realization (no ensemble averaging!) and

$$\Lambda_{\alpha\beta} = \delta_{\alpha\beta} \begin{cases} +\frac{N_r}{N_{\text{ch}}}, & \text{if } 1 \leq \alpha \leq N_l; \\ -\frac{N_l}{N_{\text{ch}}}, & \text{if } N_l < \alpha \leq N_{\text{ch}}. \end{cases} \quad (10)$$

The scattering matrix of the system, $\hat{S}(t, t')$, is

$$\mathcal{S}_{\alpha\beta}(t, t') = \delta_{\alpha\beta} \delta(t - t') - 2\pi i \nu W_{\alpha n}^{\dagger} G_{nm}^{(R)}(t, t') W_{m\beta}, \quad (11)$$

and the Green's function $G_{nm}^{(R)}(t, t')$ is the solution to:

$$\left(i \frac{\partial}{\partial t} - \hat{H}(t) + i\pi\nu \hat{W} \hat{W}^{\dagger} \right) \hat{G}^{(R)}(t, t') = \delta(t - t'), \quad (12)$$

where the matrices \hat{H} and \hat{W} are comprised by their elements (see Eqs. (5) and (7)). An analogue of Eq.(9) was used before in the energy representation in Ref. [11].

Below we consider the special case of electrons in both leads being described by identical distribution functions $f_j(t) \equiv f(t)$. The function $f(t)$ is the Fourier transform of the Fermi–Dirac distribution function:

$$f(t) = \int_{-\infty}^{+\infty} \frac{d\omega}{2\pi} e^{i\omega t} \left\{ \frac{1}{e^{\omega/T} + 1} - \frac{1}{2} \right\} = \frac{iT}{2 \sinh \pi T t} \quad (13)$$

In this case, we can derive (see Appendix B) another formula for the current through the dot:

$$\langle I(t) \rangle = 2e i \pi \nu \text{Tr} \int \int dt_1 dt_2 f(t_1 - t_2) \quad (14)$$

$$\times \left\{ \hat{W}^{\dagger} \hat{G}^{(R)}(t, t_1) \left[\hat{H}(t_1) - \hat{H}(t_2) \right] \hat{G}^{(A)}(t_2, t) \hat{W} \Lambda \right\},$$

which is more convenient for further calculations.

We calculate the variance (mean square) of the transported charge Q through the dot. We assume, that the Hamiltonian of the dot \hat{H} in Eq.(5) is represented by a time-dependent matrix in the form:

$$\hat{H}(t) = \hat{\mathcal{H}} + \hat{V}_1 \varphi(t) + \hat{V}_2 \psi(t). \quad (15)$$

Here, the time independent part of the Hamiltonian $\hat{\mathcal{H}}$ is a random $M \times M$ matrix, which obeys Gaussian statistics with the correlator

$$\overline{\mathcal{H}_{nm} \mathcal{H}_{n'm'}^*} = \lambda \delta_{nn'} \delta_{mm'} + \lambda' \delta_{mn'} \delta_{nm'}, \quad (16)$$

where $\overline{(\dots)}$ means averaging over ensemble of matrices $\hat{\mathcal{H}}$, $\lambda = M(\delta_1/\pi)^2$ and $\lambda' = \lambda(1 - g_h/4M)$, and g_h defines the crossover from orthogonal ($g_h = 0$) to unitary ($g_h = 4M$) ensembles. The parameter g_h has the meaning of the dephasing rate due to an external magnetic field in units of the level spacing δ_1 , [10,12]. It can be estimated as $g_h \simeq g_{\text{dot}} (\Phi/\Phi_0)^2$ where Φ is the magnetic flux through the dot and $\Phi_0 = hc/e$ is the flux quantum. The time dependent perturbation is described by symmetric $M \times M$ matrices, \hat{V}_i , and the time dependent functions $\varphi(t)$ and $\psi(t)$.

We make the simplifying assumption that the matrices \hat{V} are traceless $\text{Tr} \hat{V} = 0$. In this case, the unknown parameters C_{ij} are defined as

$$C_{ij} = \frac{\pi}{M^2 \delta_1} \text{Tr} \hat{V}_i \hat{V}_j, \quad (17)$$

where we used the fact that the matrix \hat{V} is symmetric. (We note that according to the definition of Eq.(17), C has dimension of energy.) The parameters C are also related to the typical value of the level velocities which characterize the evolution of an energy level $\epsilon_{\nu}(\mathbf{X})$ under the external perturbation $\mathbf{X} \hat{V}$, [13]:

$$\frac{2\delta_1}{\pi} C_{ij} = \frac{\overline{\partial \epsilon_{\nu}}}{\partial X_i} \frac{\overline{\partial \epsilon_{\nu}}}{\partial X_j} - \frac{\overline{\partial \epsilon_{\nu}}}{\partial X_i} \frac{\overline{\partial \epsilon_{\nu}}}{\partial X_j}. \quad (18)$$

Since all other responses (e.g., parametric dependence of the conductance of the dot) are expressed in terms of universal functions of the same parameters C_{ij} [13], they can be found from independent measurements. Calculations can be generalized to the case in which the trace of the perturbation matrix is not zero. See, e.g. [3].

For reflectionless contacts, the ensemble averaged scattering matrix $\overline{\mathcal{S}_{\alpha\beta}}$ is zero. This condition determines the factors Γ_n in Eq. (7):

$$\Gamma_n = \sqrt{\frac{M \delta_1}{\pi^2 \nu}}. \quad (19)$$

The ensemble average of the transmitted charge Q , defined by Eq.(1), is zero: $\overline{Q} = 0$. We calculate the second order correlator with respect to an ensemble of random matrices, Eq. (16):

$$\overline{Q^2} = \int_0^{T_p} \int_0^{T_p} dt dt' \overline{\langle I(t) \rangle \langle I(t') \rangle}. \quad (20)$$

For this purpose we use a diagrammatic technique, which has been applied to a similar class of problems. See Refs.

[3,14]. Here we present the basic elements of the diagrams which will appear in sections III and V. The ensemble averaged Green's function $G_{nm}^{R,A}$ in the absence of perturbations is equal to

$$\overline{G_{nm}^{R,A}}(\epsilon) = \pm \frac{\delta_{mn}}{i\sqrt{\lambda M}} \begin{cases} 1 + \frac{N_{\text{ch}} \pm i\epsilon}{4M}, & N_{\text{ch}} < n \leq M; \\ \frac{1}{2}, & 1 \leq n \leq N_{\text{ch}}. \end{cases} \quad (21)$$

Above we introduced the dimensionless energy, ϵ , measured in units of $\sqrt{\lambda/4M} = \delta_1/2\pi$. We expanded these Green's functions in ϵ/M and N_{ch}/M , since only those terms survive the thermodynamic limit $M \rightarrow \infty$. For the same reason, in the expression for $G_n^{(R)}$ with $n \leq N_{\text{ch}}$ one has to neglect such terms since the contribution of these elements to the final result is already of the order of N_{ch}/M .

The other element of the diagram technique used in the paper is an amputated average of the products of two Green's functions (see Fig.2(b)), called the diffuson $\mathcal{D}(t_1, t_2, \tau)$ and defined by

$$\begin{aligned} & \overline{(G_{nm}^{(R)}(t_1^+, t_2^+) G_{mn}^{(A)}(t_2^-, t_1^-))}_{\text{amp}} \\ &= 4M\lambda\mathcal{D}\left(\frac{t_1^+ + t_1^-}{2}, \frac{t_2^+ + t_2^-}{2}, t_1^+ - t_2^+\right) \\ & \times \delta(t_1^+ - t_2^+ - t_1^- + t_2^-) \end{aligned} \quad (22)$$

We can use this relation since the time arguments of diffusion satisfy $t_1^+ - t_2^+ = t_1^- - t_2^-$. Introducing new variables $t_{1,2} = (t_{1,2}^+ + t_{1,2}^-)/2$ and $\tau = t_{1,2}^+ - t_{1,2}^-$ we obtain the following equation for the diffuson $\mathcal{D}(t_1, t_2, \tau)$:

$$\begin{aligned} & \left[\frac{\partial}{\partial t_1} + \mathcal{K}_{\mathcal{D}}(t_1, \tau) \right] \mathcal{D}(t_1, t_2, \tau) = \delta(t_1 - t_2), \\ & \mathcal{K}_{\mathcal{D}}(t, \tau) = N_{\text{ch}} + \Phi^T(t, \tau) \hat{C} \Phi(t, \tau), \end{aligned} \quad (23)$$

where

$$\Phi(t, \tau) = \begin{pmatrix} \phi\left(t + \frac{\tau}{2}\right) - \phi\left(t - \frac{\tau}{2}\right) \\ \psi\left(t + \frac{\tau}{2}\right) - \psi\left(t - \frac{\tau}{2}\right) \end{pmatrix}. \quad (24)$$

The solution to the above equation is

$$\mathcal{D}(t_1, t_2, \tau) = \Theta(t_1 - t_2) \exp\left(-\int_{t_2}^{t_1} \mathcal{K}_{\mathcal{D}}(t, \tau) dt\right). \quad (25)$$

Equations (23)–(25) are written in dimensionless variables, so that energy and time are measured in units of $\delta_1/2\pi$ and $2\pi/\delta_1$ respectively. Below, intermediate expressions are also written in terms of dimensionless energy and time variables, while the final answers are represented in terms of physical quantities.

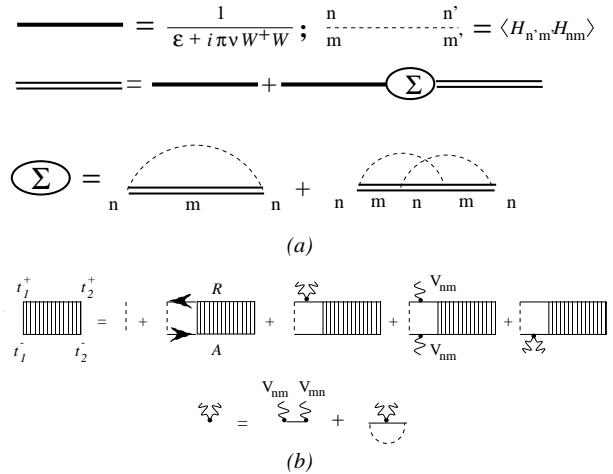


FIG. 2. (a) Diagrams for the ensemble averaged Green's function. The second term in the self-energy includes an intersection of dashed lines and is as small as $1/M$. (b) The Dyson type equation for the diffuson, $\mathcal{D}(t_1^+, t_1^-, t_2^+, t_2^-)$.

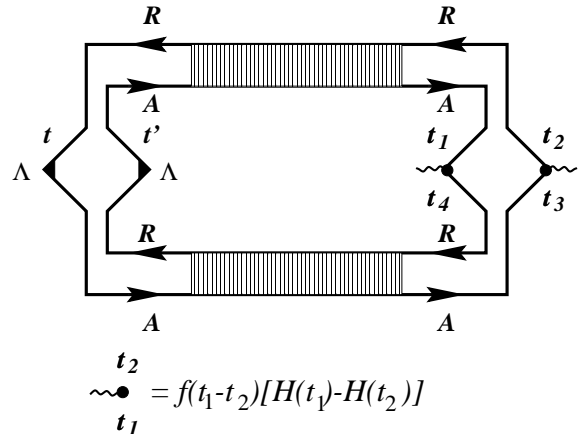


FIG. 3. The diagram representing the contribution to the charge correlator, $\overline{Q^2}$ at high temperature T .

III. MESOSCOPIC FLUCTUATIONS OF THE CURRENT AT HIGH TEMPERATURES

In this section we will consider the high temperature limit, in which the frequency of the perturbation is much smaller than the temperature. (More accurate definition of the high temperature limit is given in Sec. V.) In this case the only contribution to the charge correlation function, $\overline{Q^2}$, is given by the diagram shown in Fig. 3. The corresponding analytical expression is

$$\overline{Q^2} = 4e^2g \int_0^{2\pi} dx dy \mathcal{R}(x, y) \int_0^{+\infty} d\theta \int_{-\theta}^{\theta} d\tau F^2(\tau)$$

$$\begin{aligned} & \times \mathcal{D}\left(\frac{x+y}{2\omega} + \theta, \frac{x+y}{2\omega} + \tau, \frac{x-y}{\omega}\right) \\ & \times \mathcal{D}\left(\frac{x+y}{2\omega} + \theta, \frac{x+y}{2\omega} - \tau, \frac{x-y}{\omega}\right), \end{aligned} \quad (26)$$

where

$$\begin{aligned} \mathcal{R}(x, y) = & C_{11} \sin x \sin y + C_{22} \sin(x + \phi) \sin(y + \phi) \\ & + C_{12} (\sin(x + \phi) \sin y + \sin x \sin(y + \phi)), \end{aligned} \quad (27)$$

$$g = \frac{N_1 N_r}{N_{\text{ch}}} \quad (28)$$

is the dimensionless conductance through the dot from the left to right leads and

$$F(\tau) = \frac{T\tau}{\sinh 2\pi T\tau}. \quad (29)$$

Expression (26) can be computed for different values of parameters. In Fig. 4 we present the result of computation of $\overline{Q^2}$ for two frequencies $\omega = 0.1\gamma_{\text{esc}}$ and $\omega = \gamma_{\text{esc}}$. Both those curves exhibit C_1^2 and $\sqrt{C_1}$ dependences at weak and strong pumping respectively. We also show the analytical curve given by Eq.(37) for the $\omega \rightarrow \infty$ limit. Below we discuss different limits of Eq.(26)

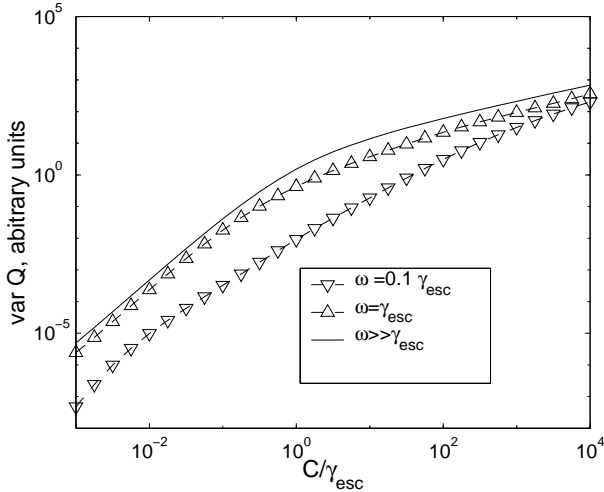


FIG. 4. The amplitude dependence of the pumped charge for different values of the frequency of the pump. For $\omega \geq \gamma_{\text{esc}}$ the curves have the C^2 dependence at small values of C and the \sqrt{C} dependence at $C \gg \gamma_{\text{esc}}$. For small frequency (e.g. $\omega = 0.1\gamma_{\text{esc}}$) there is an intermediate regime.

A. Bilinear response

First we consider the weak perturbation and perform an expansion of the diffusons up to terms linear in C_{ij} . As a result we obtain:

$$\begin{aligned} \overline{Q^2} = & 4\pi^2 e^2 g \int_0^\infty d\theta e^{-2N_{\text{ch}}\theta} \int_{-\theta}^{+\theta} d\tau F^2(\tau) \\ & \times \frac{C_1^2(2\omega\theta - \sin 2\omega\theta) + C_c^2 \sin 2\omega\theta}{\omega}, \end{aligned} \quad (30)$$

where we have introduced the linear and circular pumping amplitudes

$$C_1 = C_{11} + 2C_{12} \cos \phi + C_{22}, \quad (31)$$

$$C_c = 2 \sin \phi \sqrt{C_{11}C_{22} - C_{12}^2}. \quad (32)$$

In the case of temperature T larger than the escape rate $\gamma_{\text{esc}} = N_{\text{ch}}\delta_1/2\pi$, ($T \gg \gamma_{\text{esc}}$) we find

$$\overline{Q^2} = \frac{e^2}{24} g \frac{\delta_1}{T} \frac{1}{\gamma_{\text{esc}}^2 + \omega^2} \left(\frac{\omega^2}{\gamma_{\text{esc}}^2} C_1^2 + C_c^2 \right). \quad (33)$$

The second term of Eq.(33) survives the limit $\omega \rightarrow 0$, thus reproducing the known result for adiabatic pumping [1,3]. On the other hand, this term vanishes at high frequency. The linear term is quadratic in frequency at small frequency and tends to a constant at large frequency.

The linear pumping amplitude C_1 in the case of two pumps has the form of Eq.(31), which implies that the amplitude is just a vector sum of different pumps in the parameter space. On the other hand the circular amplitude is related to the area in the parameter space, covered by the pumps.

B. Low frequencies

Equation (26) in the adiabatic limit $\omega \rightarrow 0$ is in agreement with the results of Ref. [3]. Namely, this expression gives the same asymptotic behavior for the limits of weak and strong pumping. To demonstrate this we consider the special case of the \hat{C} matrix having the form $C_{11} = C_{22} = C$ and $C_{12} = 0$. In this case we obtain

$$\overline{Q^2} = \frac{1}{12} e^2 g \frac{\delta_1}{T} \frac{2C + (\gamma_{\text{esc}} - \sqrt{\gamma_{\text{esc}}(\gamma_{\text{esc}} + 4C)})}{\sqrt{\gamma_{\text{esc}}(\gamma_{\text{esc}} + 4C)}}. \quad (34)$$

As temperature drops down to $T \sim \gamma_{\text{esc}} = N_{\text{ch}}\delta_1/2\pi$, the variance of the transmitted charge saturates to

$$\overline{Q^2} = \frac{2}{\pi} e^2 g \frac{\delta_1}{\gamma_{\text{esc}}} \frac{C^2}{\sqrt{\gamma_{\text{esc}}(\gamma_{\text{esc}} + 4C)^3}} \quad (35)$$

The authors of Ref. [3] showed that for strong pumping the mean square transported charge is proportional to the length of the contour in the parameter space, and does not depend on the particular shape of the contour. Equations (34) and (35) support this statement, since for $C \gg \gamma_{\text{esc}}$ they reproduce a \sqrt{C} dependence on the pumping amplitude. In the opposite case of weak pumping Eqs. (34) and (35) give C^2 dependence in accordance

with [1,2]. To understand the strong pumping dependence, we consider a loop in the parameter space. See Fig.(5). We notice (see Eq.(42)) and Refs. [1,3], that adiabatic pumping can be related to a contour integral in the parameter space. At sufficiently strong pumping the system at distant points of this space is uncorrelated and the total contribution to the pumped charge comes from the uncorrelated pieces of the loop, being proportional to their number.

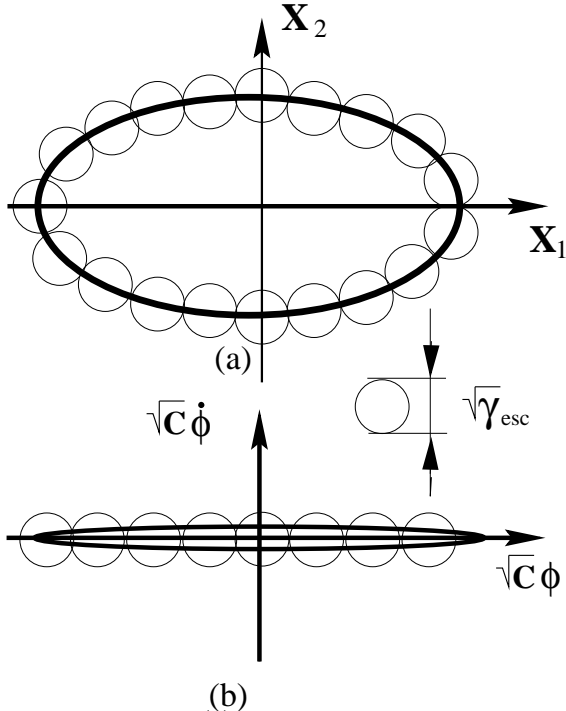


FIG. 5. In figure (a) a loop is shown in the parameter plane. The grid divides the plane onto pieces, so that parts of the loop in the different pieces give uncorrelated contributions to the transported charge. Figure (b) shows the loop in the phase space for strong pumping. In this case the loop can be divided onto pairs, and the pairs are not correlated. On the other hand parts of the loop of one pair are close to each other, so they are strongly correlated.

In the limit of low frequency and zero C_c (single pump), the mean square fluctuation of the charge per cycle is quadratic in frequency. For weak pumping the amplitude of charge fluctuations is determined by Eq.(33) with $\phi = 0$ for arbitrary frequency ω . (For a single pump, C_1 is the only parameter.) For strong pumping (but still $\omega^2 C_1 \ll \gamma_{\text{esc}}^3$) we find

$$\overline{Q^2} = \frac{25}{576\pi} e^2 g \frac{\omega^2}{\gamma_{\text{esc}}^2} \frac{\delta_1}{T} \left(\frac{C_1}{\gamma_{\text{esc}}} \right)^{3/2}. \quad (36)$$

We explain this dependence on the amplitude of the perturbation in the next section.

C. High frequencies

In the limit of high frequencies, $T \gg \omega \gg \gamma_{\text{esc}}$, the variance of the transmitted charge is given by

$$\overline{Q^2} = \frac{1}{12} e^2 g \frac{\delta_1}{T} \frac{C_1 + \gamma_{\text{esc}} - \sqrt{\gamma_{\text{esc}}(\gamma_{\text{esc}} + 2C_1)}}{\sqrt{\gamma_{\text{esc}}(\gamma_{\text{esc}} + 2C_1)}}. \quad (37)$$

In the limit of strong pumping this expression has the $\sqrt{C_1}$ asymptotic behavior. The curve Eq.(37) is represented in Fig. 4 by the solid line.

IV. PHOTOVOLTAIC EFFECT AS PUMPING IN PHASE SPACE

In this section we discuss the mechanism of charge transport by a single pump at finite frequencies (*i.e.* the irreversible contribution to the d.c.-current). We show the similarity with the mechanism of adiabatic charge pumping, discussed in [1]. In the adiabatic approximation the system's motion is considered in a parameter space. For finite frequencies the parameter space has to be extended to phase space, which contains not only the perturbation parameters but also their time derivatives.

According to Eq. (9), the transported charge for one period is determined by

$$Q = e \int_0^{T_p} dt \int dt' \int d\tau \int \frac{d\epsilon}{2\pi} e^{i\epsilon\tau} f(\tau) \quad (38)$$

$$\times \text{Tr} \left\{ \mathcal{S} \left(\epsilon, \frac{t+t'}{2} + \frac{\tau}{4} \right) \mathcal{S}^\dagger \left(\epsilon, \frac{t+t'}{2} - \frac{\tau}{4} \right) \Lambda \right\}.$$

We use the Wigner transform for the scattering matrix:

$$\mathcal{S}(t, t') = \int \mathcal{S}(\epsilon, (t+t')/2) e^{i\epsilon(t-t')} \frac{d\epsilon}{2\pi}. \quad (39)$$

We consider charge pumping at high temperature ($T \gg \omega$). In this case the integration over τ is limited by the inverse temperature $1/T$. On the other hand, the scattering matrix $\mathcal{S}(\epsilon, t)$ in the Wigner representation varies slowly with respect to its time argument t . This allows us to expand the scattering matrices in Eq.(38) to linear order in τ . Using the unitarity of the scattering matrix we finally obtain

$$Q = e \int_0^{T_p} dt \int \frac{d\epsilon}{2\pi} \frac{1}{\cosh^2 \epsilon/2T} \quad (40)$$

$$\times \text{Tr} \left\{ \Lambda \left(\frac{\partial \mathcal{S}(\epsilon, t)}{\partial t} \mathcal{S}^\dagger(\epsilon, t) - \mathcal{S}(\epsilon, t) \frac{\partial \mathcal{S}^\dagger(\epsilon, t)}{\partial t} \right) \right\}$$

This equation was used by Brouwer in [1]. (See also [11]). The scattering matrix in the Wigner representation is a function of the perturbation itself and its higher order derivatives with respect to time. (See Appendix C.) In the adiabatic approximation the derivatives are neglected as being small to higher orders in frequency. Beyond the

adiabatic approximation, we have to include the derivatives.

We demonstrate that the analysis of Ref. [1] can be applied to our case. We assume, that there is a single parameter $\varphi(t)$. Then, following Brouwer, Ref. [1], we introduce a vector field

$$P_i(\epsilon, t) = \text{Im Tr} \left\{ \Lambda \frac{\partial \mathcal{S}(\epsilon, t)}{\partial X_i} \mathcal{S}^\dagger(\epsilon, t) \right\}, \quad (41)$$

where $X_i = d^i \varphi(t)/dt^i$ and i is a non-negative integer.

In these notations Eq.(40) for the transported charge Q is given by

$$Q = e \oint \int \frac{d\epsilon}{2\pi} \frac{1}{\cosh^2 \epsilon/2T} \sum_{i=0}^{\infty} P_i(\epsilon) dX_i. \quad (42)$$

The loop integral in the above equation can be rewritten as a surface integral using Stoke's theorem. We develop our analysis for the transported charge to the lowest order in frequency, so that the scattering matrix depends only on $X_0 = \varphi(t)$ and $X_1 = \dot{\varphi}(t)$. According to Stoke's theorem for this two dimensional space, we obtain

$$Q = e \int \frac{d\epsilon}{2\pi} \frac{1}{\cosh^2 \epsilon/2T} \int d\varphi d\dot{\varphi} \Pi(\epsilon), \quad (43)$$

$$\Pi(\epsilon) = \text{Im Tr} \left\{ \Lambda \frac{\partial \mathcal{S}(\epsilon)}{\partial \varphi} \frac{\partial \mathcal{S}^\dagger(\epsilon)}{\partial \dot{\varphi}} \right\}.$$

In appendix C we present a formal derivation of $\partial \mathcal{S}/\partial \dot{\varphi}$ from the equation of motion, Eq.(12), in terms of the Green's functions of the dot to lowest order in $\omega/\gamma_{\text{esc}}$.

Now we interpret results found in the previous section using Eq.(43). For weak pumping we keep the time dependent perturbation to lowest order to calculate the derivatives with respect to φ and $\dot{\varphi}$. Then we consider $\Pi(\epsilon)$ to be a constant and the integral over φ and $\dot{\varphi}$ gives the area of the contour in phase space. For a harmonic field $\varphi(t) = \cos \omega t$, the contour is an ellipse with large semiaxis \sqrt{C} , small semiaxis $\omega\sqrt{C}$ and area $\pi\omega C$. For the variance of the transmitted charge, we expect $\overline{Q^2} \propto \omega^2 C^2/\gamma_{\text{esc}}^4$, which is in agreement with Eq.(33) for $\omega \ll \gamma_{\text{esc}}$.

In the limit of low frequency but strong pumping, we can apply Eq.(43) to understand Eq.(36). The power dependence $[C^{3/2}]$ is different from the adiabatic case $[C^{1/2}]$. The loop in phase plane is long along the φ axis but narrow in the $\dot{\varphi}$ direction because the frequency is small. [See Fig. 5(b).] The charge variation is determined by a sum of independent contributions from pieces of the contour along the φ axis. As can be seen from Fig. 5(b) the number of the independent pieces is $N_{\text{ind}} = \sqrt{C/\gamma_{\text{esc}}}$. In the $\dot{\varphi}$ direction the system is correlated inside each piece of the contour since all points along the $\dot{\varphi}$ direction are separated by a distance, smaller than the correlation length. The characteristic area S_c of each part is proportional to $\omega\sqrt{C\gamma_{\text{esc}}}$. The variance of the transported charge can thus be estimated as

$$\overline{Q^2} \propto e^2 N_{\text{ind}} S_c^2 \propto e^2 \frac{\omega^2}{\gamma_{\text{esc}}^2} \left(\frac{C}{\gamma_{\text{esc}}} \right)^{3/2}. \quad (44)$$

When the amplitude of the field C or the frequency ω increases further, so that $\omega^2 C_1 \geq \gamma_{\text{esc}}^3$, this picture is no longer valid. The trajectory does not have parts close to each other and each part gives an independent contribution. The situation is similar to the case of strong adiabatic pumping, as shown in Fig. 5(a) and discussed in [3]. The variance of the transported charge is proportional to the total number of uncorrelated parts, so that $\overline{Q^2} \propto \sqrt{C}$, see Eq. (37).

V. LOW TEMPERATURE

The previous discussion of d.c.-current generation is quite general. However, it does not take into account the heating of electrons by an external field which becomes important at low temperature. In this regime, the electron distribution function in the dot changes and acquires a width larger than the electron temperature in the leads.

The new width T_h of the distribution function can be estimated from the following picture. An electron has random transitions between different energy levels. The time between consecutive transitions t_{tr} is determined by the Fermi golden rule:

$$t_{\text{tr}}^{-1} = \sum_m 2\pi |V_{nm}|^2 \delta(\epsilon_n - \epsilon_m \pm \omega) \sim \overline{|V_{nm}|^2} / \delta_1 = \frac{C}{\pi}. \quad (45)$$

The first equality sign follows from the Fermi golden rule, the second sign represents an estimate of the characteristic value of the matrix elements $\overline{|V_{nm}|^2}$ and the density of states $1/\delta_1$, the last equation is the definition of C , cf. Eq.(17). Since an electron stays in the dot for a time $\tau_{\text{esc}} = \gamma_{\text{esc}}^{-1} = 2\pi/N_{\text{ch}}\delta_1$, it performs $N_{\text{tr}} = 1/t_{\text{tr}}\gamma_{\text{esc}} = C/\gamma_{\text{esc}}$ transitions. Each transition changes the energy of the electron by ω . As in the random walk problem, the displacement of electrons in energy space is $\propto \omega\sqrt{C/\gamma_{\text{esc}}}$.

This analysis gives a new temperature scale T_h :

$$T_h = \omega \sqrt{\frac{C}{\gamma_{\text{esc}}}}. \quad (46)$$

This scale has a meaning only for strong fields, $C \gg \gamma_{\text{esc}}$, so that the diffusion picture in energy space is valid. Otherwise, electrons experience few transitions with change of energy ω . Now we consider low temperatures, so that $T \gg T_h$ is not valid. We calculate the fluctuations of d.c. current for a system with a single pump. As we know

from Sec. III, at high frequency the number of pumps is not important and the result depends on their linear combination.

Unlike the diagram, shown in Fig. 3, diagrams presented in Fig. 6 have additional diffusons dressed on the distribution functions $f(\tau)$. Collecting diagrams in Fig. 3 and Fig. 6 we obtain the following expression for the variance of the pumped charge:

$$\begin{aligned}
\overline{Q^2} &= 4e^2 C N_{\text{ch}} g \int_0^{T_p} dt dt' \int_0^\infty d\theta \int_{-\theta}^{+\theta} d\tau \tilde{F}^2(\tau) \\
&\times \mathcal{D}\left(\frac{t+t'}{2} + \theta, \frac{t+t'}{2} + \tau, t-t'\right) \\
&\times \mathcal{D}\left(\frac{t+t'}{2} + \theta, \frac{t+t'}{2} - \tau, t-t'\right) \\
&\times \int_0^{+\infty} d\xi \mathcal{D}(t, t-\xi, 2\tau) \int_0^{+\infty} d\xi' \mathcal{D}(t', t'-\xi', 2\tau) \\
&\times \{2C \sin^2 \omega(t-\xi) \sin^2 \omega(t'-\xi') \sin^2 \omega\tau \\
&\quad + N_{\text{ch}} \sin \omega t \sin \omega t'\}
\end{aligned} \tag{47}$$

where g is the dimensionless conductance of the dot (see Eq.(28)) and

$$\tilde{F}(\tau) = \frac{T \sin \omega\tau}{\sinh 2\pi T\tau}. \tag{48}$$

At high temperature $T \gg \omega$ Eq.(47) reduces to Eq.(26). Indeed, all three diagrams in Fig. 6 are smaller than the diagram in Fig. 3 at least by one factor ω/T .

Now we discuss the limit of high frequency $\omega \gg \max\{\gamma_{\text{esc}}, C\}$. This inequality allows us to perform integration over ξ and ξ' in Eq.(47). We can replace $\sin^2 \omega(t-\xi)$ by $1/2$ and use the approximation

$$\int_0^\infty \mathcal{D}(t, t-\xi, 2\tau) d\xi \approx \frac{1}{N_{\text{ch}} + 2C \sin^2 \omega\tau}. \tag{49}$$

In this limit the product of the diffusons in the second and third lines of Eq.(47) does not depend on τ .

Energy of an electron in the dot changes due to the external field resulting in the redistribution of the electrons in the energy space. The new distribution function becomes wider than that of electrons in the leads at temperature T . Consequently, the Fourier transform of the electron distribution function becomes narrower. The right hand side of Eq.(49) represent the effect of heating. This function appears in the integral over τ in Eq.(47) along with the function $F(\tau)$, defined by Eq.(29). At sufficiently low temperature the convergence of the integral over τ is determined by the 'heating factors', Eq.(49) rather than by $F(\tau)$. We note, that the shape of the new distribution function is not a Fermi function with a higher temperature. Instead, its Fourier transform has the form of the right hand side of Eq. (49).

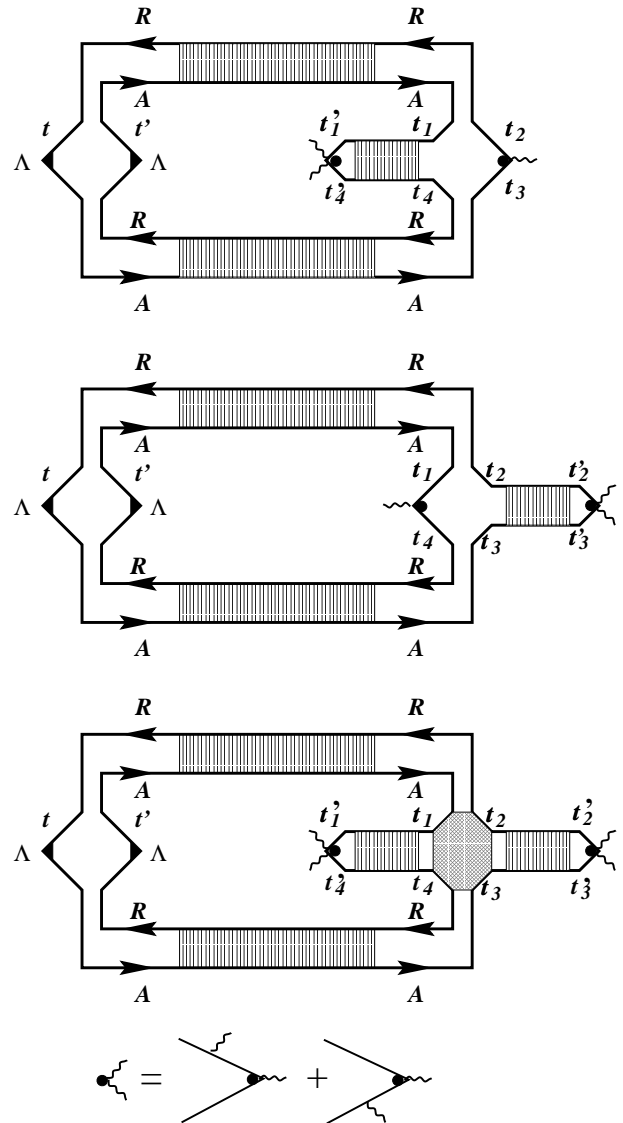


FIG. 6. Diagrams, which contribute to the d.c.-current at low temperature limit. (We do not show diagrams, which can be obtained from the above by omitting the upper or lower diffusons.) The last diagram contains the Hikami box, which is presented in Fig. 7.

To be more specific, we consider the strong pumping limit $C \gg \gamma_{\text{esc}}$, when the electron distribution function is determined by the new scale T_h , see Eq.(46). We find

$$\overline{Q^2} = \frac{3}{16} e^2 g \frac{\delta_1}{\omega}. \tag{50}$$

The same parameter dependence can be found from Eq.(37) replacing temperature T by the new energy scale T_h .

Equation (47) has two terms. One term contains factor $\sin \omega t \sin \omega t'$. This term survives the high temperature limit, see Sec. III. Nonetheless at low temperature the heating modifies the results of Sec. III, so that the temperature dependence saturates at the characteristic temperature scale T_h .

The second term was completely neglected in the previous sections. The origin of this term is similar to that of the thermoelectric effect in a conductor out of thermodynamic equilibrium. Although electrons are in equilibrium in the leads, the heating changes their distribution function in the dot, producing a non-equilibrium distribution. Then non-equilibrium electrons escape from the dot. The direction of each escape is determined by the realization of the dot. An unbalance between electrons escaping through the left or right leads gives current. ($\sin^2 \omega \tau$ term in Eq. (47) reflects the electron-hole asymmetry, necessary for thermoelectric effects.)

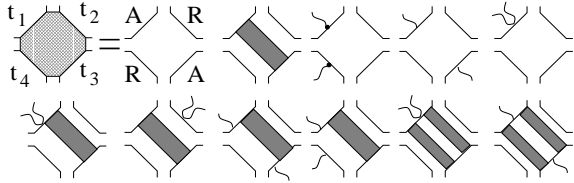


FIG. 7. The Hikami box, introduced in Fig. 6, can be obtained from these diagrams as well from their rotations. The grey rectangulars represent averages of the type $\overline{G^{(R)}G^{(R)}}$ and $\overline{G^{(A)}G^{(A)}}$.

VI. CONCLUSIONS

We studied the d.c.-current through the quantum dot generated *e.g.* by time-dependent distortions of the dot shape. This d.c.-current is fluctuating from sample to sample and we found the second moment of its distribution. Unlike the previous works [1,3] on the adiabatic pumping we treated the system for a broad range of external frequencies thus providing a bridge between adiabatic pumping and photovoltaic effects in microjunctions of Ref. [5].

The adiabatic approximation is not valid when the frequency of the perturbation ω is comparable with the escape rate from the dot γ_{esc} . Beyond the adiabatic approximation the d.c.-current consists of reversible and irreversible parts. The reversible contribution was studied in the adiabatic regime. This contribution is determined by an integral over the contour in parameter space. On the other hand the irreversible contribution to the d.c.-current is determined by an integral over this contour in phase space.

A crossover from the bilinear (C^2) to \sqrt{C} regime was found in [3]. The crossover happens when the system makes a large loop during one period of the external field, so that it is uncorrelated at different points of the loop, see Fig. 5(a). We showed, that this crossover is universal and happens at arbitrary frequency. This result is consistent with the representation of the d.c.-current as an integral along the contour in the phase space. An intermediate regime exists for a single pump at low frequency and moderate amplitude of the external field. This regime is

described by a $C^{3/2}$ dependence of the variance of the d.c.-current on the field amplitude.

We also considered a wide temperature range. At high temperature the variance of the current decreases as T^{-1} . We found that at low temperature heating becomes important and it introduces a characteristic temperature T_h , see Eq. (46), below which the temperature dependence of the d.c.-current saturates. The result of heating on the d.c.-current is twofold. The first effect diminishes the d.c.-current by broadening of the electron distribution function. The second effect produces the a thermoelectric field, and is a non-equilibrium effect. This effect is related to the electron-hole asymmetry in the dot. Our results are different from the observed experimentally temperature dependence, see also Ref. [3].

Finally, the photovoltaic effect is not symmetric with respect to inversion of magnetic field, similarly to adiabatic pumping case, see Ref. [3].

We are thankful to P. W. Brouwer for useful discussions. The work was supported by Cornell Center for Materials Research under NSF grant No. DMR-9632275 (M.G.V. and V.A.) and Packard Fellowship (I.L.A.).

APPENDIX A:

We define the wave function of electrons in channel α moving towards the dots by $\psi_\alpha(x, t)$ with $x < 0$, where $|x|$ determines the distance from the dot boundary, see Fig. (8). Then $\psi_\alpha(x, t)$ for $x > 0$ represents the outgoing electrons. The boundary $x = 0$ is described by a superposition of the incoming and outgoing electron states and we denote it by $\psi_\alpha(0, t)$. The wave function of electrons in state i is denoted by $\psi_i(t)$.

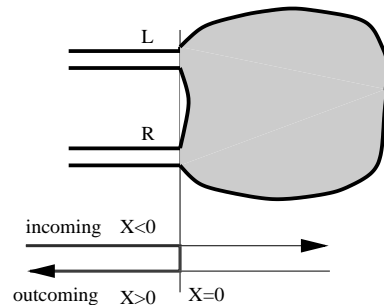


FIG. 8. Correspondence between the sign of x and the direction of motion of electrons with respect to the dot.

We introduce the Keldysh Green's functions

$$\hat{\mathcal{G}}_{\alpha\beta}(t, t', x, x') = \quad (A1)$$

$$\begin{pmatrix} \mathcal{G}_{\alpha\beta}^{(R)}(t, t', x, x') & \mathcal{G}_{\alpha\beta}^{(K)}(t, t', x, x') \\ 0 & \mathcal{G}_{\alpha\beta}^{(A)}(t, t', x, x') \end{pmatrix},$$

$$\hat{\mathcal{G}}_{i\alpha}(t, t', x') = \begin{pmatrix} \mathcal{G}_{i\alpha}^{(R)}(t, t', x') & \mathcal{G}_{i\alpha}^{(K)}(t, t', x') \\ 0 & \mathcal{G}_{i\alpha}^{(A)}(t, t', x') \end{pmatrix}, \quad (A2)$$

which are defined in terms of

$$\begin{aligned}\mathcal{G}_{\alpha\beta}^{(R)}(t, t', x, x') &= -i\Theta(t-t')\langle[\psi_\alpha(x, t), \psi_\beta^\dagger(x', t')]_+\rangle, \\ \mathcal{G}_{\alpha\beta}^{(A)}(t, t', x, x') &= i\Theta(t'-t)\langle[\psi_\alpha(x, t), \psi_\beta^\dagger(x', t')]_+\rangle, \\ \mathcal{G}_{\alpha\beta}^{(K)}(t, t', x, x') &= -i\langle[\psi_\alpha(x, t), \psi_\beta^\dagger(x', t')]_-\rangle,\end{aligned}$$

where $[\cdot, \cdot]_\pm$ denote commutator and anticommutator respectively. The similar expressions can be written down for $\hat{\mathcal{G}}_{i\alpha}(t, t', x')$ Green's function, with $\psi_\alpha(x, t)$ replaced by $\psi_i(t)$.

We assume that electrons do not interact in the reservoirs and the Green's function of the incoming electrons ($x; x' < 0$) is given by the Keldysh structure:

$$\begin{aligned}\mathcal{G}_{\alpha\beta}(t, t', x, x') & \quad (\text{A3}) \\ = & \begin{pmatrix} G_{\alpha\beta}^{(R)}(t-t', x-x') & G_{\alpha\beta}^{(K)}(t-t', x-x') \\ 0 & G_{\alpha\beta}^{(A)}(t-t', x-x') \end{pmatrix},\end{aligned}$$

where

$$G_{\alpha\beta}^{(R)}(t, x) = i\Theta(t) \delta_{\alpha\beta} \delta(v_F t - x), \quad (\text{A4})$$

$$G_{\alpha\beta}^{(A)}(t, x) = -i\Theta(-t) \delta_{\alpha\beta} \delta(v_F t - x), \quad (\text{A5})$$

$$G_{\alpha\beta}^{(K)}(\epsilon, x) = \tilde{f}_\alpha(\epsilon) \left(G_{\alpha\beta}^{(R)}(\epsilon, x) - G_{\alpha\beta}^{(A)}(\epsilon, x) \right), \quad (\text{A6})$$

where $\tilde{f}(\epsilon)$ is the distribution function of electrons in the channel α . In equilibrium with temperature T ,

$$\tilde{f}_\alpha(\epsilon) = \tanh \frac{\epsilon - \delta\mu_\alpha}{2T}, \quad (\text{A7})$$

where $\delta\mu_\alpha$ represent relative change in chemical potential for different leads.

The equations of motion for the Green's functions defined by Eqs. (A1) and (A2) have the form:

$$i \left[\frac{\partial}{\partial t} - v_F \frac{\partial}{\partial x} \right] \hat{\mathcal{G}}_{\alpha\beta}(t, t', x, x') \quad (\text{A8})$$

$$= \delta(x) W_{\alpha i} \hat{\mathcal{G}}_{i\beta}(t, t', x') + \delta(t-t') \delta(x-x') \hat{1},$$

$$\left[i \frac{\partial}{\partial t} - H_{ij}(t) \right] \hat{\mathcal{G}}_{j\alpha}(t, t', x') \quad (\text{A9})$$

$$= W_{i\beta}^\dagger \hat{\mathcal{G}}_{\beta\alpha}(t, t', 0, x').$$

We notice that due to causality, $G_{\alpha\beta}^{(A)}(t, t', 0, x') \equiv 0$ for $x' < 0$. This observation significantly simplifies further calculations. Indeed, we can represent the Keldysh component of the Green's function in the left hand side of Eq.(A9) in the form

$$\begin{aligned}\mathcal{G}_{i\alpha}^{(K)}(t, t', x') &= \int dt_1 \left[\frac{1}{i\partial/\partial t - \hat{H}(t)} \right]_{ij} (t, t_1) \\ &\times W_{j\beta}^\dagger \mathcal{G}_{\alpha\beta}(t_1, t', 0, x'),\end{aligned} \quad (\text{A10})$$

The corresponding advance component is zero. Here $1/(i\partial/\partial t - \hat{H}(t))$ is the retarded component of the electron Green's function in the dot. This definition is different from that given in the main part of the paper, see Eq.(10). The latter will appear naturally in the end of this section. The additional term $\sim W^\dagger W$ takes into account the escape from the dot through the leads.

The next step is to represent Eq.(A8) in the form

$$\begin{aligned}\mathcal{G}_{\alpha\beta}^{(K)}(t, t', x, x') &= G_{\alpha\beta}^{(K)}(t-t', x-x') \quad (\text{A11}) \\ + \int dt_1 dt_2 G_{\alpha\gamma}^{(R)}(t-t_1, x) &\left[W \frac{1}{i\partial/\partial t - \hat{H}(t)} W^\dagger \right]_{\gamma\delta} (t_1, t_2) \\ &\times \mathcal{G}_{\delta\beta}^{(K)}(t_2, t', 0, x')\end{aligned}$$

In the above equation we consider $x = 0$. Using $G_{\alpha\beta}^{(R)}(t-t', 0)$ from Eq.(A4) we find

$$\begin{aligned}\mathcal{G}_{\alpha\beta}^{(K)}(t, t', 0, x') &= \int dt_1 \left[1 - \hat{W} \frac{i\pi\nu}{i\partial/\partial t - \hat{H}(t)} \hat{W}^\dagger \right]_{\alpha\delta}^{-1} (t, t_1) \\ &\times G_{\delta\beta}^{(K)}(t_1, t', 0, x'), \quad x' < 0. \quad (\text{A12})\end{aligned}$$

Substituting this expression to Eq.(A11) and taking $x = +|\delta| \rightarrow 0$, we obtain for $x' < 0$:

$$\mathcal{G}_{\alpha\beta}^{(K)}(t, t', +|\delta|, x') = \int dt_1 \mathcal{S}_{\alpha\gamma}(t, t_1) G_{\gamma\beta}^{(K)}(t_1 - t', -x'), \quad (\text{A13})$$

where the scattering matrix $\mathcal{S}_{\alpha\beta}(t, t')$ is given by Eq.(11).

Equation (A13) is valid for $x' < 0$. We have to repeat the procedure described above to calculate the electron Green's function in the leads for $x' > 0$. Since the equations which determine evolution of the Green's function from $x' < 0$ to $x' > 0$ are conjugated to those for x , we conclude, that

$$\begin{aligned}\mathcal{G}_{\alpha\beta}^{(K)}(t, t', +|\delta|, +|\delta|) & \quad (\text{A14}) \\ = \int \int dt_1 dt_2 \mathcal{S}_{\alpha\gamma}(t, t_1) G_{\gamma\delta}^{(K)}(t_1 - t_2, 0) \mathcal{S}_{\delta\beta}^\dagger(t_2, t')\end{aligned}$$

The currents in the left and right leads are given by

$$I_l(t) = ev_F \quad (\text{A15})$$

$$\times \sum_{\alpha=1}^{N_l} \left(\mathcal{G}_{\alpha\alpha}^{(K)}(t, t, +|\delta|, +|\delta|) - \mathcal{G}_{\alpha\alpha}^{(K)}(t, t, -|\delta|, -|\delta|) \right)$$

$$I_r(t) = ev_F \quad (\text{A16})$$

$$\times \sum_{\alpha=N_l+1}^{N_{ch}} \left(\mathcal{G}_{\alpha\alpha}^{(K)}(t, t, +|\delta|, +|\delta|) - \mathcal{G}_{\alpha\alpha}^{(K)}(t, t, -|\delta|, -|\delta|) \right),$$

where $\delta \rightarrow 0$. This limit is just a reminder that $\mathcal{G}_{\alpha\alpha}^{(K)}(t, t, -|\delta|, -|\delta|)$ is taken for incoming electrons and is given by Eq.(A6). Consequently,

$$\mathcal{G}_{\alpha\alpha}^{(K)}(t, t, -|\delta|, -|\delta|) = f(+i0), \quad (\text{A17})$$

$$f(t) = \int_{-\infty}^{+\infty} e^{i\omega t} \tilde{f}(\omega) \frac{d\omega}{2\pi}.$$

Since the charge is conserved, $I_1(t) = -I_r(t)$. We rewrite the current through the dot as

$$I(t) = \frac{N_r I_1(t) - N_l I_r(t)}{N_{\text{ch}}} = I_1(t) = -I_r(t). \quad (\text{A18})$$

Substituting Eqs. (A14) and (A17) into Eqs. (A15) and (A16) and using Eq.(A18) we obtain Eq.(9).

APPENDIX B:

In this appendix we derive Eq.(14) from the general Eq. (13). The only assumption we are using here is that the distribution function of electrons is the same in all channels, *i.e.* $f_\alpha(t) \equiv f(t)$. Substituting the explicit form of the scattering matrix from Eq. (11), we obtain

$$\begin{aligned} I(t) = & 2\pi i \nu e \left\{ \int dt_1 f(t-t_1) \Lambda_{\alpha\beta} \left[\hat{W}^\dagger \hat{G}^{(A)}(t_1, t) \hat{W} \right]_{\beta\alpha} \right. \\ & - \int dt_1 f(t_1-t) \Lambda_{\alpha\beta} \left[\hat{W}^\dagger \hat{G}^{(R)}(t, t_1) \hat{W} \right]_{\beta\alpha} \\ & - 2\pi i \nu \int \int dt_1 dt_2 f(t_1-t_2) \Lambda_{\alpha\beta} \\ & \left. \times \left[\hat{W}^\dagger \hat{G}^{(R)}(t, t_1) \hat{W} \hat{W}^\dagger \hat{G}^{(A)}(t_2, t) \hat{W} \right]_{\beta\alpha} \right\}, \end{aligned} \quad (\text{B1})$$

where the diagonal matrix $\hat{\Lambda}$ is defined in Eq. (11), and $\hat{G}(t, t')$ denotes the Green's function in the dot.

Now we use the equation of motion of the retarded and advanced Green's functions, Eq. (12), to simplify the right hand side of Eq. (B1). For this purpose, we pre-multiply the equation for the advanced component $\hat{G}^{(A)}(t_2, t')$ by the retarded component $\hat{G}^{(A)}(t, t_1)$, then we post-multiply the transposed equation for the retarded component $\hat{G}^{(A)}(t, t_1)$ by $\hat{G}^{(A)}(t_2, t')$. Subtracting from the second equation the first one, we obtain

$$\begin{aligned} & 2\pi i \nu \hat{G}^{(R)}(t, t_1) \hat{W} \hat{W}^\dagger \hat{G}^{(A)}(t_2, t') \quad (\text{B2}) \\ & = i \left[\frac{\partial}{\partial t_1} + \frac{\partial}{\partial t_2} \right] \hat{G}^{(R)}(t, t_1) \hat{G}^{(A)}(t_2, t') \\ & + \hat{G}^{(R)}(t, t_1) \left[\hat{H}(t_1) - \hat{H}(t_2) \right] \hat{G}^{(A)}(t_2, t') \\ & - \left[\hat{G}^{(R)}(t, t_1) \delta(t_2 - t') - \delta(t - t_1) \hat{G}^{(A)}(t_2, t') \right] \end{aligned}$$

Substituting this equation to Eq. (B1) we obtain Eq.(14).

APPENDIX C:

The equation for the Green's function in the Wigner representation for a time-dependent Hamiltonian is

$$\begin{aligned} & 2\epsilon \hat{G}(\epsilon, t) - \left[H_0 - i\pi\nu \hat{W} \hat{W}^\dagger, \hat{G}(\epsilon, t) \right]_+ \quad (\text{C1}) \\ & + \sum_{k=0}^{\infty} \frac{\varphi^{(k)}(t)}{(2i)^k k!} \left\{ \hat{V} \frac{\partial^k \hat{G}(\epsilon, t)}{\partial \epsilon^k} + (-1)^k \frac{\partial^k \hat{G}(\epsilon, t)}{\partial \epsilon^k} \hat{V} \right\} = 2. \end{aligned}$$

Here $\hat{G}(\epsilon, T)$ is the Green's function in the Wigner variables ϵ and t . We represented $\hat{H}(t)$ in the form $\hat{H}(t) = \hat{H}_0 + \hat{V}\varphi(t)$.

In the adiabatic limit only the $k = 0$ is taken into account. This approximation is crucial in the case of a single pump. By appropriate choice of the beginning of the cycle the pump moves for the second half of the cycle along the same trajectory as for the first half, but in the opposite direction. As a consequence, the total transported charge Q , Eq.(40), vanishes in the adiabatic approximation. To remove this symmetry, we can add another pump oscillating with the same frequency, but with different phase shift. Also, the higher order terms in Eq.(C1) break this symmetry.

We consider contribution to the lowest order in frequency to the transported charge Q . For this purpose, we neglect all terms with $k \geq 2$, keep the $k = 1$ term to the first order and include all orders in $k = 0$ term. The solution is

$$\begin{aligned} \hat{G}_0(\epsilon, t) &= \frac{1}{\epsilon - \hat{H}_0 - \hat{V}\varphi(t) + i\pi\nu \hat{W} \hat{W}^\dagger}, \quad (\text{C2}) \\ \hat{G}_1(\epsilon, t) &= i \frac{\dot{\varphi}(t)}{2} \left(\hat{G}_0(\epsilon, t) \hat{V} \hat{G}_0^2(\epsilon, t) - \hat{G}_0^2(\epsilon, t) \hat{V} \hat{G}_0(\epsilon, t) \right). \end{aligned}$$

To the lowest order in $\dot{\varphi}(t)$, the scattering matrix $\hat{\mathcal{S}}$ has the form

$$\hat{\mathcal{S}}_1(\epsilon, t) = \hat{\mathcal{S}}_0(\epsilon, \varphi(t)) + \dot{\varphi}(t) \hat{\mathcal{A}}(\varphi(t)), \quad (\text{C3})$$

where

$$\hat{\mathcal{S}}_0(\epsilon, \varphi(t)) = 1 - 2\pi\nu \hat{W}^\dagger \hat{G}_0(\epsilon, t) \hat{W}, \quad (\text{C4})$$

and

$$\begin{aligned} \hat{\mathcal{A}}(\epsilon, t) &\equiv \frac{\partial \hat{\mathcal{S}}}{\partial \dot{\varphi}} \quad (\text{C5}) \\ &= \frac{i}{2} \left(\hat{G}_0(\epsilon, t) \hat{V} \hat{G}_0^2(\epsilon, t) - \hat{G}_0^2(\epsilon, t) \hat{V} \hat{G}_0(\epsilon, t) \right). \end{aligned}$$

[1] P. W. Brouwer, Phys. Rev. B **58**, R10135, (1998).

[2] F. Zhou, B. Spivak, and B. Altshuler, Phys. Rev. Lett., **82**, 608, (1999).

- [3] T. A. Shutenko, B. L. Altshuler and I. L. Aleiner, Phys. Rev. B, **61**, 10366, (2000).
- [4] M. Switkes, C. M. Marcus, K. Campman and A. C. Gosard, Science, **283**, 1907, (1999).
- [5] V. I. Fal'ko and D. E. Khmel'nitskii, Sov. Phys. JETP, **68**, 186, (1989).
- [6] A. A. Bykov, G. M. Gusev, and Z. D. Kvon, Sov. Phys. JETP, **70**, 742, (1990).
- [7] V. I. Belinicher and B. I. Sturman, Usp. Fiz. Nauk **130**, 415, (1980) [Sov. Phys. Usp., **23**, 199, (1980)].
- [8] P.W. Brouwer and I.L. Aleiner, Phys. Rev. Lett., **82**, 390 (1999).
- [9] A. A. Abrikosov, L. P. Gorkov, I. E. Dzyaloshinskii, *Methods of Quantum Field Theory in Statistical Physics*, (Prentice-Hall, Englewood Cliffs, NJ, 1963).
- [10] C.W.J. Beenakker, Rev. Mod. Phys, **69**, 731, (1997).
- [11] M. Büttiker, H. Thomas, and A. Pretre, Z. Phys. B, **94**, 133, (1994).
- [12] B.L. Altshuler, *et. al.*, in *Quantum Theory of Solids*, (Mir, Moscow, 1982).
- [13] B.D. Simons and B.L. Altshuler, Phys. Rev. Lett., **70**, 4063, (1993); B.L. Altshuler and B.D. Simons, in *Mesoscopic Quantum Physics*, eds. E. Akkermans *et. al.* (Elsevier, 1995).
- [14] M. G. Vavilov and I. L. Aleiner, Phys. Rev. B, **60**, R16311, (1999).